

$\pi N\sigma$ term, $\bar{s}s$ in the nucleon, and the scalar form factor: A lattice study

S. J. Dong, J.-F. Lagaë,* and K. F. Liu

Department of Physics and Astronomy, University of Kentucky, Lexington, Kentucky 40506

(Received 2 July 1996)

We report on a lattice QCD calculation of the $\pi N\sigma$ term, the scalar form factor, and $\langle N|\bar{s}s|N\rangle$. The disconnected insertion part of $\sigma_{\pi N}$ is found to be 1.8 ± 0.1 times larger than the connected insertion contribution. The q^2 dependence of $\sigma_{\pi N}(q^2)$ is about the same as $G_E(q^2)$ of the proton so that $\sigma_{\pi N}(2m_\pi^2) - \sigma_{\pi N}(0) = 6.6\pm 0.6$ MeV. The ratio $y = \langle N|\bar{s}s|N\rangle/\langle N|\bar{u}u + \bar{d}d|N\rangle = 0.36\pm 0.03$. Both results favor a $\sigma_{\pi N} \sim 53$ MeV, slightly larger than our direct calculation of $\sigma_{\pi N} = 49.7\pm 2.6$ MeV. We also compute F_s and D_s and find that the agreement with those from the octet baryon mass splittings crucially depends on the inclusion of the large disconnected insertion. Finally, we give our result for the $KN\sigma$ term. [S0556-2821(96)04521-3]

PACS number(s): 12.38.Gc, 13.75.Gx, 13.75.Jz, 14.20.Dh

Like the pion mass in the meson sector, the $\pi N\sigma$ term is a measure of the explicit chiral symmetry breaking in the baryon sector. It is considered a fundamental quantity which pertains to a wide range of issues in low-energy hadron physics, such as quark and baryon masses, strangeness content of the nucleon, pattern of SU(3) breaking, πN and KN scatterings, kaon condensate in dense matter, trace anomaly, and decoupling of heavy quarks. Defined as the double commutator of the isovector axial charge with the Hamiltonian density taken between the nucleon states, i.e.,

$$\sigma_{\pi N} = \frac{1}{3} \sum_{a=1,3} \langle N|[Q_a^5, [Q_a^5, \mathcal{H}(0)]]|N\rangle \quad (1)$$

which appears in the off-shell πN scattering amplitude [1], it has in QCD the expression

$$\sigma_{\pi N} = \hat{m} \langle N|\bar{u}u + \bar{d}d|N\rangle, \quad (2)$$

where $\hat{m} = (m_u + m_d)/2$.

It is shown [2] that at lowest order in m_π (i.e., m_π^2), it is equal to the unphysical, but on shell, isospin even πN -scattering amplitude at the Cheng-Dashen point, $\Sigma_{\pi N} = f_\pi^2 \bar{T}^+(s = m_N^2, t = q^2 = 2m_\pi^2)$. Thus, $\Sigma_{\pi N}$ can be extracted from πN -scattering experiment via fixed- t dispersion relation for instance [2]. It is further shown [3] that the next higher order term which is nonanalytic in quark mass (i.e., proportional to $\hat{m}^{3/2}$ or m_π^3) drops out if $\Sigma_{\pi N}$ is identified with $\sigma_{\pi N}(2m_\pi^2)$ [3] which is only a function of q^2 . This shows that the difference Δ_R in the relation $\Sigma_{\pi N} = \sigma_{\pi N}(2m_\pi^2) + \Delta_R$ is of the order m_π^4/m_N^4 and has been shown to be indeed negligible (~ 0.35 MeV) in a chiral perturbation calculation [3,4].

Various estimates of $\Sigma_{\pi N}$ have ranged from 22 to 110 MeV over the years, but eventually settled around 60 MeV [4]. On the other hand, a puzzle was raised by Cheng [5]. If one assumes that $\langle N|\bar{s}s|N\rangle = 0$, a reasonable assumption

from the OZI rule, the $\sigma_{\pi N}^{(0)}$ obtained from the octet baryon masses gives only 32 MeV, almost a factor 2 smaller than $\Sigma_{\pi N}$ extracted from the πN scattering. This puzzle was tackled from both ends. First, the scalar form factor was calculated [4] in chiral perturbation theory (χ PT) with the two correlated pions as the dominating intermediate state. As a result, the scalar form factor is found to be exceedingly soft which leads to a large change of $\sigma_{\pi N}(q^2)$ in a small range of q^2 , i.e., $\Delta\sigma_{\pi N} = \sigma_{\pi N}(2m_\pi^2) - \sigma_{\pi N}(0) = 15.2\pm 0.4$ MeV. Thus, this reduces $\sigma_{\pi N}$,

$$\sigma_{\pi N} = \Sigma_{\pi N} - \Delta\sigma_{\pi N}, \quad (3)$$

to ~ 45 MeV. The remaining discrepancy between $\sigma_{\pi N}$ and $\sigma_{\pi N}^{(0)}$ is reconciled if one admits the possibility of a large $\bar{s}s$ content in the nucleon [5,6]. From the pattern of SU(3) breaking in the octet baryon masses, one finds [6,5]

$$\sigma_{\pi N} = \sigma_{\pi N}^{(0)}/(1-y), \quad (4)$$

where $y = 2\langle N|\bar{s}s|N\rangle/\langle N|\bar{u}u + \bar{d}d|N\rangle$. Given $\sigma_{\pi N}^{(0)} = 32$ MeV from the octet baryon masses [5], or 35(5) MeV from the one-loop chiral perturbation theory (χ PT) calculation [6] and $\sigma_{\pi N} = 45$ MeV, Eq. (4) implies $y = 0.2-0.3$.

Hence, a consistent solution seems to have emerged which suggests that $\sigma_{\pi N} \sim 45$ MeV, $\Delta\sigma_{\pi N} \sim 15$ MeV, and $y \sim 0.2-0.3$. In this paper, we undertake a lattice QCD calculation of the above quantities to scrutinize the viability of this resolution. It turns out that our study points to a significantly different solution. Our results indicate that the scalar form factor is not as soft as envisioned in the χ PT calculation [4]. Instead of 15 MeV, we find $\Delta\sigma_{\pi N} = 6.6\pm 0.6$ MeV. We also find that $y = 0.36\pm 0.03$ which is larger than the phenomenologically deduced value above. Both of these numbers imply a larger $\sigma_{\pi N} \sim 53$ MeV. This is only one and a half σ larger than our direct calculation at 49.7(2.6) MeV. We shall argue that the direct calculation of $\sigma_{\pi N}$ is more susceptible to systematic errors than $\Delta\sigma_{\pi N}$ and y .

The calculation of $\sigma_{\pi N}$ in lattice QCD has been attempted by several groups [7,8] who employed the Feynman-Hellman theorem

*Present address: High Energy Physics Division, Argonne National Laboratory, Argonne, IL 60439.

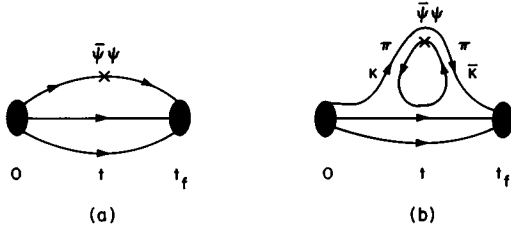


FIG. 1. (a) Connected insertion, (b) disconnected insertion.

$$\hat{m} \frac{\partial M_N}{\partial \hat{m}} = \hat{m} \langle N | \bar{u}u + \bar{d}d | N \rangle_{\text{CI}} + \hat{m} \langle N | \bar{u}u + \bar{d}d | N \rangle_{\text{DI}} \quad (5)$$

and obtained $\sigma_{\pi N}$ through the derivative of the nucleon mass. We note that in Eq. (5) the *connected insertion* (CI) part comes from the differentiation with respect to the valence quark propagator; whereas the *disconnected insertion* (DI) part comes from the derivative of the fermion determinant. Their contributions to the scalar charge $\bar{\psi}\psi$ in the nucleon are shown schematically in Fig. 1. In the DI the quark flow lines are not joined together as in the CI. They are, nonetheless, correlated via the background gauge fields which are not drawn. In the quenched approximation approach, it is found that $\sigma_{\pi N}$ obtained from the derivative of the nucleon mass is only about 15–25 MeV [7]. This is much smaller than the phenomenological value of ~ 45 MeV [4]. The smallness of $\sigma_{\pi N}$ in this case is traced to the fact that the nucleon mass in the quenched approximation is calculated with the determinant set to a constant, so that its derivative corresponds to the CI only (which is verifiable by comparing to the direct evaluation of the CI [9,10]) and it does not include DI which can be substantial. Indeed, when the derivative of M_N is calculated with dynamical fermions included, it is found [8] that the left-hand side (LHS) of Eq. (5) which now includes the DI becomes ~ 2 to 3 times larger than the CI contribution. This implies a large contribution of the DI. Since the error on $\partial M_N / \partial \hat{m}$ is quite large [10,8], we decide to calculate the DI directly [10] with the help of the Z_2 noise [11]. Following our calculation of the flavor singlet g_A^0 [12], we calculate the CI and DI of $\sigma_{\pi N}$ directly in the quenched approximation. In terms of the Feynman-Hellman theorem, it would correspond to calculating $\partial M_N / \partial \hat{m}$ by taking the derivative of the determinant first before setting it to a constant.

Lattice calculations of three-point functions have been used to study the EM [13], axial (isovector) [14], and pseudoscalar (πNN) [15] form factors, and the flavor singlet g_A^0 [12]. For the scalar form factor, we calculate the following two- and three-point functions:

$$G_{PP}^{\alpha\alpha}(t, \vec{p}) = \sum_x e^{-i\vec{p}\cdot\vec{x}} \langle 0 | \chi^\alpha(x) \bar{\chi}^\alpha(0) | 0 \rangle, \quad (6)$$

$$G_{PSP}^{\alpha\alpha}(t_f, \vec{p}, t, \vec{q}) = \sum_{x_f, x} e^{-i\vec{p}\cdot\vec{x}_f + i\vec{q}\cdot\vec{x}} \langle 0 | \chi^\alpha(x_f) S(x) \bar{\chi}^\alpha(0) | 0 \rangle, \quad (7)$$

where t and t_f indicate the time for the scalar insertion and the nucleon sink as illustrated in Fig. 1. \vec{p} is the momentum

of the nucleon at the sink and \vec{q} is the momentum transfer of the scalar density. Since we use a point source for the nucleon which contains all lattice momenta, momentum conservation will pick out the momentum $\vec{p}' = \vec{p} - \vec{q}$ for the nucleon source. χ^α is the proton interpolating field and S is the scalar density

$$S(x) = 2\kappa/8\kappa_c [\bar{u}u(x) + \bar{d}d(x)], \quad (8)$$

where we have implemented the mean-field improvement tadpole factor $8\kappa_c$ to define the lattice operator [16]. We shall calculate CI and DI separately.

The CI is calculated in the same way as the isovector axial coupling g_A^3 and its form factor $g_A^3(q^2)$ [14]. The lattice $g_{S,\text{con}}^L = \langle N | \bar{u}u + \bar{d}d | N \rangle_{\text{con}}^L$ is obtained by fitting the two- and three-point functions G_{PP} and G_{PSP} to two exponentials in the form fe^{-mt_f} and $g_{S,\text{con}}^L f e^{-mt_f}$ simultaneously, using the data-covariance matrix to account for correlations. The form factor at different momentum transfer q^2 are evaluated by taking the appropriate combination of G_{PP} and G_{PSP} in Eqs. (6) and (7): i.e.,

$$\frac{G_{PSP}^{\alpha\alpha}(t_f, \vec{p}, t, \vec{q}) G_{PP}^{\alpha\alpha}(t, \vec{p})}{G_{PP}^{\alpha\alpha}(t_f, \vec{p}) G_{PP}^{\alpha\alpha}(t, \vec{q})} \xrightarrow{t_f, t \gg a} g_{S,\text{con}}^L(q^2), \quad (9)$$

where \vec{p} is the momentum of the nucleon sink which we take to be $\vec{0}$.

Our quenched gauge configurations were generated on a $16^3 \times 24$ lattice at $\beta = 6.0$. The gauge field was thermalized for 5000 sweeps from a cold start and 24 configurations separated by at least 1000 sweeps were used. Periodic boundary conditions were imposed on the quark fields in the spatial directions. In the time direction, Dirichlet boundary conditions were imposed on the quarks to provide larger time separations than available with periodic boundary conditions. The nucleon sink and source were placed symmetrically with respect to the time boundaries so that each Z factor, the amplitude for the nucleon interpolating field to excite the ground state from the vacuum, is canceled in the ratios of correlation function in Eq. (9) [13,14]. This is in contrast with a calculation of f_π , for example, where the matrix element of the current between the pion and the vacuum is explicitly needed and could be contaminated by boundary effects. As long as the time separations t and $t_f - t$ are large enough, the form factor $g_S(q^2)$ should not depend on the nucleon interpolation field. All quark propagators were chosen to originate from lattice time slice 5; the secondary nucleon source was fixed at time slice 20 (except for $\kappa = 0.154$ where the quark propagators from time slice 3 to 22 were used). We also averaged over the directions of equivalent lattice momenta in each configuration; this reduces error bars.

We have verified that the time separation is sufficient so that there is a plateau for the scalar density insertion at time slices t after the proton ground state is achieved. This is done for the three lightest quarks with $\kappa = 0.154, 0.152, \text{ and } 0.148$ and $\vec{q}^2 a^2$ up to $4(2\pi/L)^2$. The numerical detail of this part is given in Ref. [14]. The nucleon masses M_{Na} for $\kappa = 0.154, 0.152, \text{ and } 0.148$ are 0.746(23), 0.884(15), and

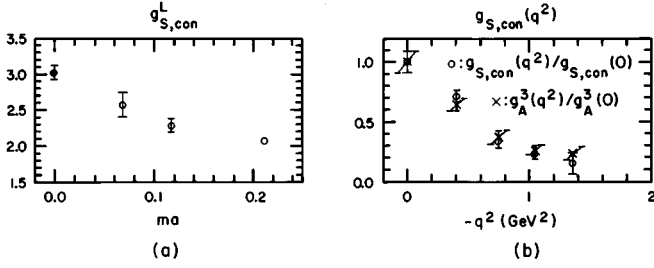


FIG. 2. (a) The lattice $g_{S,con}^L$ for the CI as a function of the quark mass ma . The chiral limit result is indicated by \bullet . (b) The form factor $g_{S,con}^L(q^2)$ at the chiral limit.

1.17(1), respectively. The corresponding pion masses $m_\pi a$ are 0.385(9), 0.493(7), and 0.689(6). Extrapolating the nucleon and pion masses to the chiral limit where we determine $\kappa_c = 0.1568(1)$ and the nucleon mass at the chiral limit to be 0.54(3). Using the nucleon mass to set the scale which we believe to be appropriate for studying nucleon properties [14,15,12], the lattice spacing $a^{-1} = 1.74(10)$ GeV is determined. The three κ 's then correspond to quark masses of about 120, 200, and 370 MeV, respectively.

Plotted in Fig. 2(a) are the lattice $g_{S,con}^L$ results. Due to the fact that the quenched χ PT calculation exhibits a leading nonanalytic behavior of $m^{3/2}$ for the nucleon mass [17], we extrapolate $g_{S,con}^L$ to the chiral limit ($\kappa_c = 0.1568$) with the form $C + Dm^{1/2}$. This is so because $g_{S,con}^L = \partial M_N / \partial \hat{m}$ in the quenched approximation as we alluded to earlier in Eq. (5). As a result, we obtain $g_{S,con}^L = 3.04(9)$ as shown in Fig. 2(a). The g_S in the continuum with the modified minimal subtraction (MS) scheme is related to its lattice counterpart by the relation $g_S = Z_S g_S^L$, where Z_S is the finite lattice renormalization constant. The one-loop calculation gives $Z_S = 0.995$ for $\beta = 6.0$ [16], from which we find $g_{S,con} = 3.02 \pm 0.09$. We also computed isovector $g_S^3 = \langle N | \bar{u}u - \bar{d}d | N \rangle$ which does not involve the DI and found it to be 0.63(7).

Since $\sigma_{\pi N}$ is renormalization group invariant, the CI contribution is $\sigma_{\pi N,con} = \hat{m} g_{S,con}^L$ where \hat{m} is the lattice quark mass. From m_π^2 and M_N , we find $\hat{m} = 5.84(13)$ MeV. Thus, $\sigma_{\pi N,con} = 17.8(9)$ MeV which agrees well with previous calculations [7,9,20]. The CI part of the form factor is obtained by extrapolating $g_{S,con}^L(q^2)$ at different κ to the chiral limit. It is plotted in Fig. 2(b) together with $g_A^3(q^2)$, the isovector axial form factor. We see that their q^2 dependence are almost identical within errors. Insofar as the concept of meson dominance goes, this reflects in part the fact that the isovector scalar meson a_0 mass and that of the axial-vector meson a_1 are close to each other in the lattice calculation. Such as in the case of the axial coupling constants [12], we also find that the ratio $R_S = g_S^3/g_{S,con}$ dips below the SU(6) result of 1/3 as the quark mass becomes lighter. This is interpreted as due to the cloud quark or antiquark effect and is responsible for the $\bar{u} - \bar{d}$ parton difference reflected in the violation of the Gottfried sum rule [21]. Only when the cloud degree of freedom is eliminated in the valence approximation [21], where the Fock space is limited to the valence, do we recover the SU(6) limit. This indirectly shows the effect of the cloud quarks in the CI.

We calculate the DI in Fig. 1(b) the same way we did for

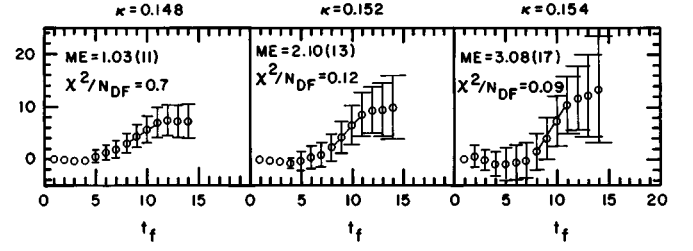


FIG. 3. The ratios of Eq. (10) for the scalar insertion are plotted for the three κ cases. ME is the fitted slope.

the DI part of g_A^0 [12] by summing over t , the insertion time slice of the scalar density. For $t_f \gg a$, this sum becomes [9,12]

$$\sum_t \frac{G_{PSP}^{\alpha\alpha}(t_f, \vec{p}, t, \vec{q}) G_{PP}^{\alpha\alpha}(t, \vec{p})}{G_{PP}^{\alpha\alpha}(t_f, \vec{p}) G_{PP}^{\alpha\alpha}(t, \vec{q})} \xrightarrow{t_f \gg a} \text{const} + t_f g_{S,dis}^L(q^2), \quad (10)$$

where \vec{p} is the momentum of the nucleon sink which we take to be $\vec{0}$. t is summed from time slices 5 to 20 (i.e., 4 time slices away from the boundary) to avoid the contamination from the fixed boundary in the time direction [12].

Thus, we calculate the sum as a function of t_f and take the slope to obtain the DI part of $g_S^L(q^2)$. Since the DI involves quark loops which entail the calculation of traces of the inverse quark matrices, we use the proven efficient algorithm to estimate these traces stochastically with the Z_2 noise [11] which was shown to be the optimal choice yielding minimal variance [22] and has been auspiciously applied to the study of g_A^0 [12].

The results of Eq. (10) with 300 complex Z_2 noise and 50 gauge configurations for $\kappa = 0.148, 0.152$, and 0.154 are presented in Fig. 3. The corresponding $g_{S,dis}^L = \langle N | \bar{u}u + \bar{d}d | N \rangle_{dis}^L$ are obtained from fitting the slopes in the region $t_f \geq 8$ where the nucleon is isolated from its excited states with the correlation among the time slices taken into account [12]. The resultant straight-line fits covering the ranges of t_f with the minimum χ^2 are plotted in Fig. 3. Finally, the errors on the fit, also shown in the figure, are obtained by jackknifing the procedure.

Plotted in Fig. 4(a) are the results of $g_{S,dis}^L$ with the same sea-quark mass as those of the valence (and cloud) quarks in the nucleon. They suggest a nonlinear behavior in the quark mass. This is enhanced by our finding of a very soft form factor [Fig. 4(b)] which is consistent with the expectations of

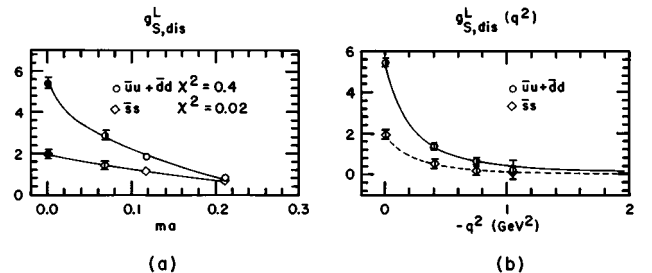


FIG. 4. (a) The DI of $\langle N | \bar{u}u + \bar{d}d | N \rangle$ and $\langle N | \bar{s}s | N \rangle$ as a function of ma . The chiral limit result is indicated by \bullet . (b) The corresponding form factors.

χ PT [6] where the pion loop leads to a nonanalytic behavior in $m_q^{3/2}$. Furthermore, this nonlinear behavior is seen prominently in hadron masses when dynamical fermions are included [23]. For these reasons, we fit $\langle N|\bar{u}u + \bar{d}d|N\rangle_{\text{dis}}$ with the constant plus $m^{1/2}$ form as for the CI and get a small χ^2 [see Fig. 4(a)]. The extrapolation to the chiral limit is carried out in the same way as in the case of g_A^0 [12]. The covariant matrix is adopted to consider the correlation among the three κ 's. The error on the chiral limit result is again obtained by jackknifing the procedure of the extrapolation. To calculate $\langle N|\bar{s}s|N\rangle$, we fix the sea-quark mass at 0.154 and extrapolate the valence-quark mass to the chiral limit with the form $C + D\sqrt{\hat{m} + m_s}$ to reflect the m_k^3 dependence of the nucleon mass from the kaon loop in χ PT. These results are also plotted in Fig. 4(a).

From Fig. 4(a), we find that $\langle N|\bar{u}u + \bar{d}d|N\rangle_{\text{dis}} = Z_S \langle N|\bar{u}u + \bar{d}d|N\rangle_{\text{dis}}^L = 5.41(15)$. This is 1.8(1) times the CI and is consistent with previous indirect calculations based on $\partial M_N / \partial \hat{m}$ with dynamical fermions [8], a direct calculation with staggered fermions [19], and the recent direct calculation [20] which gives a ratio of 2.2(6). Similarly, we find from Fig. 4(a) that $\langle N|\bar{s}s|N\rangle = Z_S f(ma) \langle N|\bar{s}s|N\rangle^L = 1.53(7)$ where we have included the finite ma correction factor $f(ma) = 0.79$ which was computed by comparing the triangle diagram in the continuum and on the lattice [18]. This is much smaller than the recent calculation [20] which gives $\langle N|\bar{s}s|N\rangle = 2.84(44)$. Part of the disagreement comes from the fact that a finite ma correction factor which is only appropriate for a CI was used in Ref. [20] for the DI. This leads to an overestimate by $\sim 30\%$. In addition, summing $\sum_{\vec{x}} S(\vec{x}, t)$ in Eq. (10) over the edges in time where the fixed boundary condition is applied as is done in Ref. [20], gives a systematic error. We find that $\langle \sum_{\vec{x}} S(\vec{x}, t) \rangle$ is a fairly uniform function of t except toward the edges of the lattice in the time direction due to the fixed boundary condition imposed there. For this reason we exclude four time slices at each of the time boundaries for both the nucleon source or sink and the $S(x, t)$ density insertion. But this unphysical boundary effect is included in Ref. [20]. In order to estimate the magnitude of the effect, we extended the density insertion to the time boundary and found $\langle N|\bar{s}s|N\rangle$ to be increased by 4%. Thus, we estimate that $\langle N|\bar{s}s|N\rangle$ in Ref. [20] to be overestimated by $\sim 35\%$. Correcting this reduces their $\langle N|\bar{s}s|N\rangle$ to 2.10(33) which is then much closer to our result. The remaining difference between this and our result of 1.53(7) may be attributable to scaling and the finite volume effect. The results of Ref. [20] are based on $12^3 \times 20$ lattices at $\beta = 5.7$; whereas ours are based on $16^3 \times 24$ lattices at $\beta = 6.0$.

From the above results, we list $\langle p|\bar{u}u + \bar{d}d|p\rangle_{\text{con}}$, $\langle p|\bar{u}u + \bar{d}d|p\rangle_{\text{dis}}$, $\langle p|\bar{u}u|p\rangle$, $\langle p|\bar{d}d|p\rangle$, $\langle N|\bar{s}s|N\rangle$, $F_S = (\langle p|\bar{u}u|p\rangle - \langle N|\bar{s}s|N\rangle)/2$, and $D_S = (\langle p|\bar{u}u|p\rangle - 2\langle p|\bar{d}d|p\rangle + \langle N|\bar{s}s|N\rangle)/2$ in Table I. We see that both D_S and F_S compare favorably with the phenomenological values obtained from the SU(3)-breaking pattern of the octet baryon masses with either linear [9,24] or quadratic mass relations [25]. Especially, we should point out that the agreement is significantly improved from the valence-quark model which predicts $F_S < 1$ and $D_S = 0$ and also those of the CI

TABLE I. Scalar contents, $\Delta\sigma_{\pi N}$, y , and $\sigma_{\pi N}$ in comparison with phenomenology.

	Lattice	Phenomenology
$\langle p \bar{u}u + \bar{d}d p\rangle_{\text{con}}$	3.02(9)	
$\langle p \bar{u}u + \bar{d}d p\rangle_{\text{dis}}$	5.41(15)	
$\langle p \bar{u}u p\rangle$	4.53(16)	
$\langle p \bar{d}d p\rangle$	3.90(16)	
$\langle N \bar{s}s N\rangle$	1.53(7)	
F_S	1.51(12)	1.52 [9,24]–1.81 [25]
D_S	-0.88(28)	-0.52 [9,24]–0.57 [25]
$\langle r^2 \rangle_S^{1/2}(ud)$	0.85(4) fm	
$\langle r^2 \rangle_S^{1/2}(s)$	1.06(9) fm	
$\Delta\sigma_{\pi N}$	6.61(59) MeV	15.2(4) MeV [4]
y	0.36(3)	0.2–0.3 [4]
$\sigma_{\pi N}$	49.7(2.6) MeV	45 MeV [4]
σ_{KN}	362(13) MeV	395 MeV [26]

alone [9,24]. The latter yields $F_S = 0.91(13)$ and $D_S = -0.28(10)$ which are only half of the phenomenological values [9,24,25]. This underscores the importance of the sea-quark contributions. We also obtain the form factor $g_{S,\text{dis}}^L(q^2) = \langle N|\bar{u}u + \bar{d}d|N\rangle_{\text{dis}}^L(q^2)$ for the DI as plotted in Fig. 4(b). We see that it is exceedingly soft which is reminiscent of the two- π intermediate state in the χ PT calculation [4]. This possibility can be seen in Fig. 1(b) with the two π intermediate state depicted. Indeed, if we assume that the DI part completely saturates $\sigma_{\pi N}$ with $g_S = 8.43(24)$, it would give $\Delta\sigma_{\pi N} = 11.5(2.1)$ MeV similar to that of the χ PT calculation [4]. However, there is also the CI part [Fig. 2(b)] which is much harder than the DI. When combined, it yields a scalar form factor $g_S(q^2)$ which is softer than $g_A^3(q^2)$ and becomes close to $G_E(q^2)$ of the proton. They are plotted in Fig. 5 for comparison. Fitting the $g_S(q^2)$ to a dipole form gives a dipole mass $m_D = 0.80(4)$ GeV. This predicts $\Delta\sigma_{\pi N} = 6.6(6)$ MeV, much smaller than the 15.2(4) MeV obtained solely based on the two- π dominance. We conclude from this that the χ PT calculation [4] is relevant to the DI but missed the CI which may be dominated by the scalar

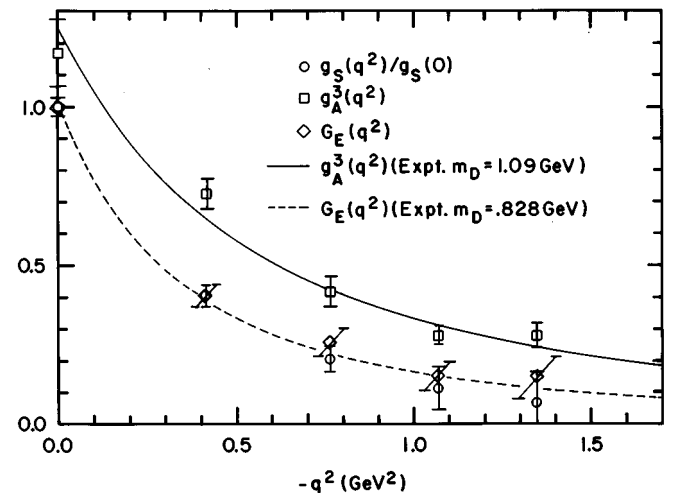


FIG. 5. The normalized form factor $g_S(q^2)/g_S(0)$ compared with $G_E(q^2)$ and $g_A^3(q^2)$ and their respective experimental results.

meson. On the other hand, the $\langle N|\bar{s}s|N\rangle(q^2)$ comes only from the DI, hence it is very soft. Its rms radius $\langle r^2 \rangle_S^{1/2}(\bar{s}s) = 1.06(9)$ fm can be interpreted as the size of the $K\bar{K}$ meson cloud in the scalar channel [see Fig. 1(b)].

For the parameter y in Eq. (4), we find it to be 0.36(3). Both $\Delta\sigma_{\pi N}$ and y differ significantly from the phenomenological solution based on χ PT as mentioned earlier which did not take into account the CI with a possible scalar dominance. This points to a higher $\sigma_{\pi N}$ than 45 MeV. Our result of $\Delta\sigma_{\pi N} = 6.6(6)$ MeV suggests a higher $\sigma_{\pi N} = \Sigma_{\pi N} - \Delta\sigma_{\pi N} \sim 53$ MeV from Eq. (3), assuming $\Sigma_{\pi N} \sim 60$ MeV. This is further enhanced by the finding of a larger y . Given $\sigma^{(0)} \sim 32$ MeV from the octet baryon masses [5], or 35(5) MeV from the one-loop χ PT calculation [6], our result of $y = 0.36(3)$ also puts $\sigma_{\pi N}$ to be around 53 MeV from Eq. (4).

Now, we turn to our result of $\sigma_{\pi N}$. Our direct calculation gives $\langle N|\bar{u}u + \bar{d}d|N\rangle = 8.43(24)$ and $\sigma_{\pi N} = 49.7(2.6)$ MeV. This is about one and a half σ smaller than 53 MeV inferred from $\Delta\sigma_{\pi N}$ and y . Since the direct computation of $\sigma_{\pi N}$ involves the determination of the quark mass which is more susceptible to systematic errors (such as the extrapolation in the quark mass and the continuum limit) than the q^2 dependence of the form factor and the ratio y , we believe that our result on $\sigma_{\pi N}$ is less reliable than $\Delta\sigma_{\pi N}$ and y . To examine the sensitivity of these three quantities as far as the chiral limit extrapolation is concerned, we fit them to a linear function in m instead of $m^{1/2}$ and find that $\Delta\sigma_{\pi N} = 4.7(8)$ MeV, $y = 0.42(3)$, and $\sigma_{\pi N} = 39.0(2.0)$ MeV. Again, we see that both $\Delta\sigma_{\pi N}$ and y favor a higher $\sigma_{\pi N} \sim 55$ MeV which is

very close to the above estimate of 53 MeV with the $m^{1/2}$ extrapolation. Yet, the directly calculated $\sigma_{\pi N}$ falls short of this expectation and is also much smaller than that of the $m^{1/2}$ extrapolation.

Clearly, calculations on larger lattices, smaller lattice spacings, and smaller quark masses will be needed to bring the systematic errors under control and obtain a completely consistent solution on $\Delta\sigma_{\pi N}, y$, and $\sigma_{\pi N}$. Eventually, dynamical fermions need to be included to complete the picture. Nevertheless, based on what we have on a qualitative and semiquantitative level, we find that a consistent solution might be close to $\Delta\sigma_{\pi N} = 6.6(6)$ MeV, $y = 0.36(3)$, and $\sigma_{\pi N} \sim 53$ MeV which are significantly different from the present phenomenological values. We should stress that our results on F_S and D_S , like their counterparts in the axial couplings, agree well with those deduced from the SU(3)-breaking pattern of the octet baryon masses and that the DI is the important ingredient for this agreement. In addition, we report the $KN\sigma$ term $\sigma_{KN} = (\hat{m} + m_s)\langle N|\bar{u}u + \bar{d}d + 2\bar{s}s|N\rangle/4$ in Table I. If we assume that they are similarly depressed as in $\sigma_{\pi N}$, we would then predict the final σ_{KN} at 389(14) MeV. It agrees with $\sigma_{KN} = 395$ MeV from a recent chiral analysis of KN scattering [26]. Finally, we note that $m_s\langle N|\bar{s}s|N\rangle = 183(8)$ MeV. Together with the kinetic and potential energy contribution of -90 MeV [27], the strange quark contributes about 90 MeV to the nucleon mass.

This work was partially supported by U.S. DOE Grant No. DE-FG05-84ER40154. The authors wish to thank G. E. Brown, N. Christ, T. Draper, and M. Rho for helpful comments.

-
- [1] S. Weinberg, Phys. Rev. Lett. **17**, 616 (1966).
[2] T. P. Cheng and R. Dashen, Phys. Rev. Lett. **26**, 594 (1971).
[3] J. Gasser, M. E. Sainio, and A. Švarc, Nucl. Phys. **B307**, 779 (1988); L. S. Brown, W. J. Pardee, and R. D. Peccei, Phys. Rev. D **4**, 2801 (1971).
[4] J. Gasser, H. Leutwyler, and M. E. Sainio, Phys. Lett. B **253**, 252 (1991); **253**, 260 (1991).
[5] T. P. Cheng, Phys. Rev. D **13**, 2161 (1976); **38**, 2869 (1988).
[6] J. Gasser and H. Leutwyler, Phys. Rep. **87**, 77 (1982); J. F. Donoghue and C. R. Nappi, Phys. Lett. **168B**, 105 (1986).
[7] S. Güsken *et al.*, Phys. Lett. B **212**, 216 (1988); P. Bacilieri *et al.*, *ibid.* **214**, 115 (1988); S. Cabasino *et al.*, *ibid.* **258**, 195 (1991).
[8] R. Gupta *et al.*, Phys. Rev. D **44**, 3272 (1991); C. Bernard *et al.*, *ibid.* **48**, 4419 (1993).
[9] L. Maiani *et al.*, Nucl. Phys. **B293**, 420 (1987).
[10] S. J. Dong and K. F. Liu, in *Lattice '91*, Proceedings of the International Symposium, Tsukuba, Japan, edited by M. Fukugita *et al.* [Nucl. Phys. B (Proc. Suppl.) **26**, 353 (1992)].
[11] S. J. Dong and K. F. Liu, Phys. Lett. B **328**, 130 (1994).
[12] S. J. Dong, J.-F. Lagaë, and K. F. Liu, Phys. Rev. Lett. **75**, 2096 (1995).
[13] T. Draper, R. M. Woloshyn, and K. F. Liu, Phys. Lett. B **234**, 121 (1990); W. Wilcox, T. Draper, and K. F. Liu, Phys. Rev. D **46**, 1109 (1992).
[14] K. F. Liu, S. J. Dong, T. Draper, J. M. Wu, and W. Wilcox, Phys. Rev. D **49**, 4755 (1994).
[15] K. F. Liu, S. J. Dong, T. Draper, and W. Wilcox, Phys. Rev. Lett. **74**, 2172 (1995).
[16] G. P. Lepage and P. B. Mackenzie, Phys. Rev. D **48**, 2250 (1993).
[17] J. Labrenz and S. Sharpe, in *Lattice '93*, Proceedings of the International Symposium, Dallas, Texas, edited by T. Draper *et al.* [Nucl. Phys. B (Proc. Suppl.) **34**, 335 (1994)].
[18] J. F. Lagaë and K. F. Liu, Phys. Rev. D **52**, 4042 (1995).
[19] R. Altmeyer, M. Göckler, R. Horsley, E. Laermann, and G. Schierholz, in *Lattice '93* [17], p. 376.
[20] M. Fukugita, Y. Kuramashi, M. Okawa, and A. Ukawa, Phys. Rev. D **51**, 5319 (1995).
[21] K. F. Liu and S. J. Dong, Phys. Rev. Lett. **72**, 1790 (1994).
[22] S. Bernardson, P. McCarty, and C. Thron, Comput. Phys. Commun. **78**, 256 (1994).
[23] S. Collins, R. G. Edwards, U. M. Heller, and J. Sloan, in *Lattice '95*, Proceedings of the International Symposium, Melbourne, Australia, edited by T. Kieu *et al.* [Nucl. Phys. B (Proc. Suppl.) **47**, 378 (1996)].
[24] M. Okawa, in *Lattice '95*, Ref. [23], p. 160.
[25] J. Gasser, Ann. Phys. (N.Y.) **136**, 62 (1981).
[26] C. H. Lee, G. E. Brown, D. P. Min, and M. Rho, Nucl. Phys. **A585**, 401 (1995).
[27] X. Ji, Phys. Rev. Lett. **74**, 1071 (1995).